5

Manufacture and design of composite grids

S.W. TSAI, K.S. LIU AND P.M. MANNE

5.1 Introduction

Composite materials technology has emerged as the darling of many industries over the past 30 years. This class of materials is light, corrosion and fatigue resistant and can be manufactured in a variety of methods. Most successes can be found in sporting goods and satellites where graphite composites are the dominant materials. Here performance is the primary goal. Other notable achievements include components of aircraft, and many industrial applications where corrosion is critical.

Composite materials have the potential to increase their market size significantly. As artificial fibers have all but replaced natural ones, we see composites as the structural materials of the future because they have unlimited supply and require less energy to process than metallic materials. There are many inhibitors to the growth of composites. They come from technological, economical and government regulatory sources. Maturing of any technology takes time, particularly if the technology involves public safety; however, innovation and favorable government regulation can hasten this process.

Composite grids form the theme for this chapter. Grids are fundamentally different from stiffened and sandwich constructions in that the load transfer mechanisms are different. Grids can be made by the widely available filament winding and pultrusion. We believe that both high performance and low cost can be achieved.

Current manufacturing processes of composite materials and structures are based on weaving, braiding, pultrusion and/or lamination. They require expensive facilities, and costly manufacturing equipment and processes. As a result, processing costs are many times the material cost. We intend to show that the cost of manufacturing composite grids can be reduced to the level of materials cost. Such composite structures can then compete against most traditional materials.

Grids are like the skeleton of a human body or the frame of old airplanes made of wood and cloth cover. The grid is the primary load-carrying

member. Skins or covers are there for another function. Optimally grids are formed by a network of ribs made of unidirectional composites. These ribs are many times stronger and lighter than metallic materials. The key is to exploit the unidirectional properties. While concrete and metallic grids have been made, their performance is limited because the ribs are isotropic. Only when ribs are unidirectional can the true potential of grids be realized. We will show how to capitalize on this principle and combine it with low-cost manufacturing.

Grid structures are not new; they have been used in civil engineering for many years. The aeronautical industry used metallic grids as early as in World War II, for example in the British Vickers Wellington bomber. The grid was metallic and offered exceptional battle damage tolerance. This extra assurance made it the favorite among the flight crew. Nowadays, jet engine covers and some hulls of the International Space Station feature integral grids machined from aluminum plates. Based on our understanding, these applications do not constitute a very effective use of grids. On the other hand, Airbus A330 and A340 have composite grid reinforced skins in their horizontal and vertical tails. Presumably they are cost effective. They are, however, hand-made. Our interest lies in developing new automatable manufacturing processes. It is hoped that with these processes, the outstanding performance of composite grids can be achieved at an affordable cost.

5.2 Grid description

We wish to describe the geometric and material characteristics of grids and show why composite grids are unique.

5.2.1 Rib orientation

Since grids have directionally dependent properties, we chose to adopt terms analogous to those commonly used for laminated composite materials. In Fig. 5.1, grids are described based on the orientations of their ribs: square, angle and $\pi/3$ isogrids, respectively. In this figure all ribs are assumed to be in the same plane and to have the same height. But that restriction is not always followed: for example, ribs may run in different planes, like plies in a laminate. All grids shown here have identical rib intersections or joints. In particular the $\pi/3$ grid is isotropic and is often called an isogrid.

5.2.2 Rib construction

There are at least two ways of making grids. The wrong way is to start with a slab of material and produce a grid by machining. As illustrated on the

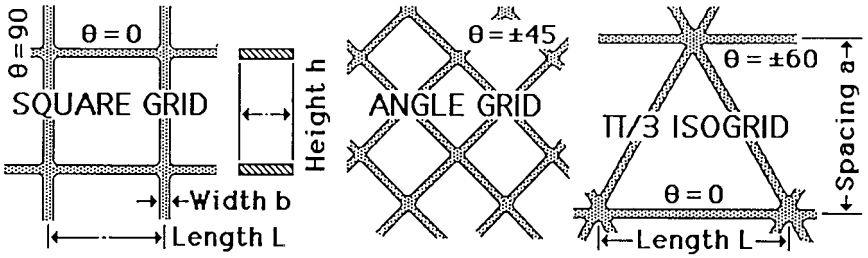

5.1 Designation of grids by rib orientation, analogous to laminated composites.

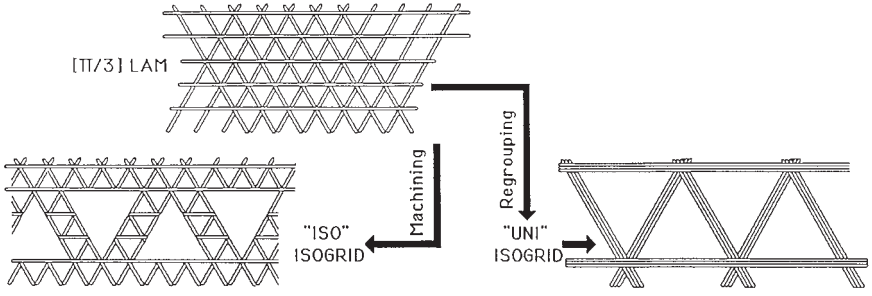

5.2 Two ways of making grids. Left: the wrong way, by machining a quasi-isotropic laminate. Right: the correct way, by forming unidirectional ribs.

left in Fig. 5.2, a quasi-isotropic laminate is taken as starting material and machined into an isogrid. We call the resulting grid an 'iso' isogrid, indicating that the starting material is isotropic. This class of grids is very costly and a very poor utilization of the material. The rib has the same stiffness as the starting material.

The right way is to use directional materials such as composites. Instead of machining, unidirectional fibers are rearranged or regrouped to form unidirectional ribs as shown on the right of Fig. 5.2. We call this class of grids 'uni' isogrids. Here the superior stiffness of unidirectional composites is fully utilized. We will show later that the 'uni' isogrids are nearly three times stiffer than the 'iso' isogrids made from the same composite materials. This is indeed the right way. For the same reason, metallic grids are not effective. In fact, there is a close relation between composite laminates and composite grids. Grids can be viewed simply as a special case of laminates, and this will be used in deriving the stiffness and strength of grids.

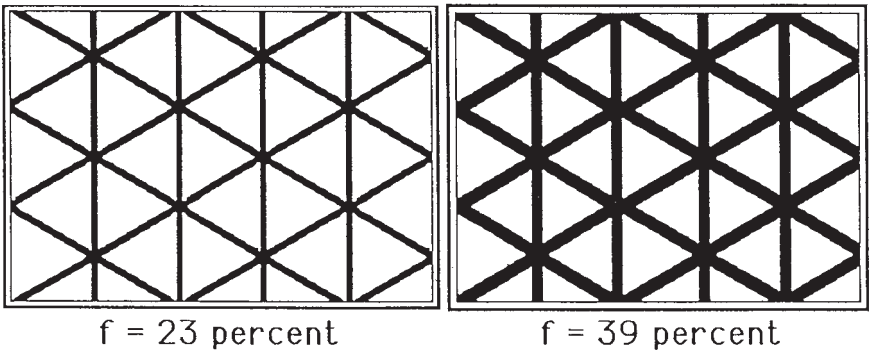

5.3 Rib volume fractions of sparse and dense grids.

5.2.3 Rib geometric parameters

The principal geometric parameters of grids are the length L, width b and height h of the ribs. A useful dimensionless measure is the rib area fraction f within a unit cell. This fraction is related to the length and width of the ribs and their orientations in the grid. Two values of f are shown in Fig. 5.3: for a sparse grid on the left and for a dense grid on the right. A dense grid can also be called a waffle plate, characterized by the fact that its ribs would not buckle.

The value of f is the same as the rib volume fraction as long as the grid pattern remains constant along the grid height. The rib fraction is analogous to the fiber volume fraction of a composite material. But fiber fraction in composite plies is not a common design variable because such a fraction is often predetermined by material suppliers. For grids, however, rib fraction is an important design variable and must be deliberately selected for a given design. We recommend f-values in the range shown in Fig. 5.3.

Rib height h is also a critical design parameter, in determining flexural rigidity in particular. A low height-to-width ratio or h/b is a shallow grid; a high ratio, a tall grid. We assume in the present work that this ratio is higher than 1. Euler buckling of ribs occurs only in the lateral direction. It is then governed by the length-to-width ratio, L/b. Such a failure mode must be compared with failure by compressive strength. Whichever is lower will be the controlling failure mode.

The relation defining the area fraction f of a grid is a function of the grid configuration. In Fig. 5.4, we show the definition of f for iso- and square grids. A visual presentation of an isogrid compared with square grids is featured. All grids have the same rib width. The smaller square grid on the left has the same area fraction f, whereas the larger square grid on the right has

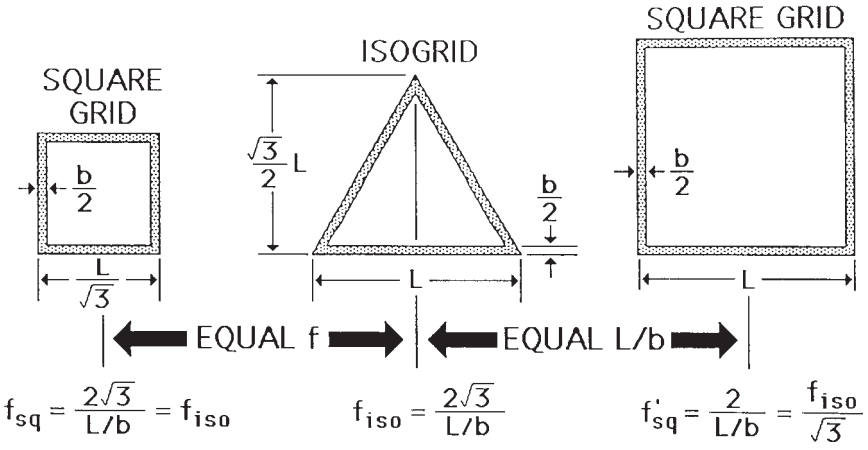

5.4 Definition of area fraction f of iso- and square grids. Slenderness ratio L/b is related to Euler buckling of ribs.

the same slenderness ratio L/b as the actual isogrid. For the smaller square grid, the length L is reduced by $\sqrt{3}$; for the larger square grid, the area fraction f is reduced by $\sqrt{3}$.

While there is a one-to-one relation between fraction f and L/b, each serves its own purpose in the design of composite grids. Area fraction f can be treated as a material property that governs both in-plane and flexural stiffnesses in a consistent manner. Slenderness ratio, L/b, is useful in its direct relation to Euler buckling of the ribs. We prefer the use of area fraction f because it reflects the weight and amount of material used in a grid.

Another geometric parameter of grids is their height or height-to-width ratio, h/b. Grids have characteristics similar to those of solid and sandwich panels. The ribs of a grid should be as tall as possible, i.e. having a high height-to-width ratio. Like plates, flexural rigidity increases with the cube of the height. Short or shallow ribs are not effective. For sandwich panels, flexural rigidity depends on both the height of the core and the laminated face sheets. If a grid has one or two face sheets, its flexural rigidity is like that of a sandwich panel. The rigidity factors are more numerous than for a grid without facing.

5.3 Manufacturing processes

Composite grids have been explored in the former Soviet republic, South Africa, Germany as well as in the USA for over 20 years. In the USA, James Koury of the USAF Phillips Laboratory (now retired), Larry Rehfield of Georgia Institute of Technology (now with the University of California,

Davis) and McDonnell Douglas Astronautics Company [1] have been pioneering the use of aluminum and later composite grids principally for the fairing and the interstage cone of missiles. W. Brandt Goldsworthy of Rolling Hills, California, pioneered not only pultruded but also filament wound grids. He first proposed this for the Beechcraft Star Ship in the 1970s.

Recently, Burt Rutan of Scaled Composites in Mojave, California, built the fuselage of a corporate jet out of composite grids. The USAF continues to explore composite grids with new applications. The McDonnell Douglas Handbook [1] has been updated with the use of composite materials by Chen and Tsai [2] and by Huybrechts [3]. The modeling used in this work draws heavily from these earlier publications. The software developed by these authors is instrumental in the analysis and figures used throughout the current effort.

It has been recognized by many people that filament winding would be an optimal method for manufacturing grids if the composite tows could be guided by some soft tooling. Grids are assembled by carving out slots or grooves in a rubber tool.

5.3.1 Assembly methods

We believe that new approaches can improve performance and, at the same time, lower cost. A variation in the grid assembly is the configuration of the rib intersection or joint. Three possible joints are shown in Fig. 5.5.

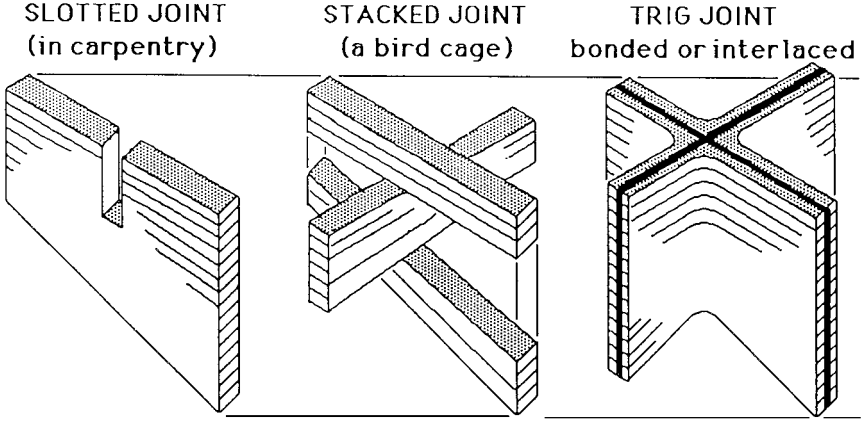

5.5 Three types of joints in a grid. The slotted joint is not recommended. Stacked and TRIG joints can be produced more easily and have better properties.

Slotted joint grids

The traditional slotted joint grids are shown on the left in Fig. 5.5 and are most frequently used in carpentry. Slots are cut into ribs and assembled. The disadvantages of this design include:

- cost of machining slots,
- difficult assembly of many ribs having multiple slots,
- low rib strength introduced by machined slots and notches,
- low grid stiffness and strength from imperfect fit at slotted joints.

We understand that Composite Optics Incorporated of San Diego, California, used [π/3] laminates as the rib in order to increase the rib strength. The use of laminates for ribs, however, degrades the grid stiffness by a factor of 3 from unidirectional ribs. It is therefore our opinion that slotted joint grids should remain as a popular technique for carpenters and cabinet makers.

Stacked joint grids

We believe that the stacked joint grids shown in the middle in Fig. 5.5 can be as effective as slotted joint grids and can be simpler to manufacture. An example of stacked joint grid is the bird cage, which has been in existence for centuries. To build a stacked grid, longitudinal and hoop or cross members are stacked. Members run on separate planes, similarly to the plies in laminate. There are at least two variations. The longitudinal members (longis) are pultruded, filament wound or made in a female mold by blow molding. The cross members (circs) can be skins applied by filament winding to form a circular or conical grid or shell.

The longitudinal tubes may be fan-shaped, for example, and serve the same purpose as a sandwich core between the inner and outer filament wound skins. Although winding can also have a helical pattern if an increase in shear rigidity is desired, such a process increases the cost of manufacturing over pure hoop winding. The longitudinal and cross members may be fully or partially populated, i.e. the longis do not have to be placed adjacent to one another. The hoop wound plies can be continuous or discontinuous like bands or rings. An example of a ring reinforced cylinder is shown in Fig. 5.6.

Other examples of a stacked grid include cross-members made by molding or vacuum infiltration. A multi-hole bar or ring through which longitudinal rods or tubes are threaded and bonded forms a bird cage-like structure. There are many possible configurations for different applications. Stacked grids, however, are currently limited to orthogrids. Isogrids, for example, are difficult to make because ribs in three levels must be stacked and joined.

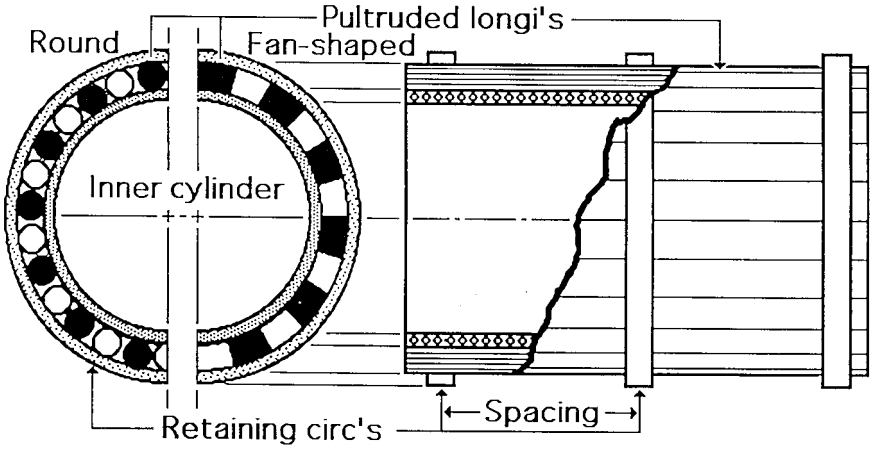

5.6 A stacked grid with round or fan-shaped longitudinal members sandwiched between inner and outer windings.

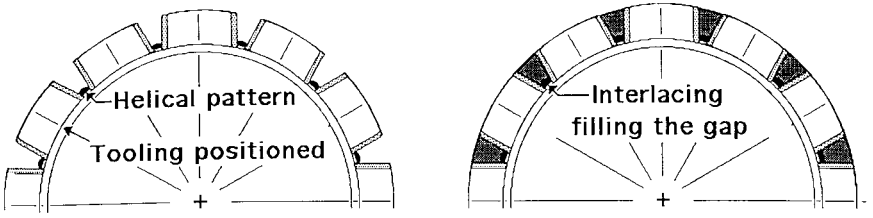

5.7 A filament wound cylinder made by the TRIG process. Left: tooling from contoured tubes. Right: wound interlacing fills the V-shaped grooves for grid strength.

Interlaced joint grids

For the interlaced grid, the thin wall tubes, again, are the starting components. The filament wound tubes with all-hoop plies provide maximum stiffness for the final grid. The tubes are sliced to a contour that fits a mandrel. They are then positioned as tooling on the mandrel. This is shown on the left in Fig. 5.7. The V-shaped gaps between tooling are filled with interlacing tows, as shown on the right. The interlacing tows carry sufficient resin to bond the tooling and interlacing together to form a solid, continuous rib. The interlacing gives superior strength to the grid. The tooling becomes part of the finished grid and provides high stiffness to the grid. Although tooling contributes to the grid stiffness, it terminates at the rib joints. The discontinuity is small relative to the length of the rib. The effect on the grid stiffness is small.

Significant cost savings can be obtained when the interlacing is filament wound with one helical winding angle. Having a V-shaped groove along a helical pattern would allow high-speed winding. That would further reduce the cost of assembly.

5.3.2 Features of grids

We have discovered theoretically that grids are more efficient if the ribs are tall and thin. This process, identified as the tooling reinforced interlaced grid (TRIG), yields a high geometric definition for the ribs and also high grid stiffness. Several current interlacing and fiber placement processes use rubber or foam as guide and tooling. These processes do not produce the high definition and stiffness that the TRIG process does.

The advantages of composite grids are derived from the availability of mass-producible rods and tubes, and from the final assembly by filament winding. This winding process is one of the most advanced and widely available processes. Curing is done at room or elevated temperature. Debulking, bagging and autoclaving are not required. With this process the cost of making a grid can be close to the cost of materials, not many times the cost. Assembly by adhesive bonding in the case of some stacked grids can also be cost effective.

Although the stiffness of composite grids is nearly equal to that of laminates, the strength is many times higher. This is because unidirectional ribs do not fail by microcracking or delamination, but by loss of strength or buckling. Where foamed tubes are used, the grids will have superior damping and acoustic properties that cannot be matched by metallic structures. Composite grids are also more resilient. There is no permanent deformation upon unloading. Thus composite grids do not dent or crumple like sheet metals.

While the advantages of composite grids are high strength and low cost, there are also disadvantages. As of now, grids can only be made in simple geometric shapes. Such a limitation is often imposed by filament winding. Circular and conical shells are the easiest. Spherical shells can be done using the TRIG process. But doubly curved or concave surfaces are not suitable for grids. Bolting is not recommended without local reinforcement.

Finally we recommend that grids be designed to carry all the loads. Skins are present for functional reasons only: in sandwich panels the skins carry the load.

5.4 Mechanical properties of grids

We wish to describe the stiffness and strength of grids and compare them with comparable properties of laminates.

5.4.1 Stiffness of quasi-isotropic laminates

It is useful to compare the stiffness of laminates and equivalent grids. The simplest comparison is that between isotropic laminates and isogrids. Laminates become quasi-isotropic with equally spaced ply orientations of [π/3], [π/4], [π/5] and so on. Similarly isotropy of the grid is assured when the three ribs are spaced 60° apart. There are closed-form solutions of the plane stress stiffness components [4].

The quasi-isotropic invariants are linear combinations or the ply stiffness components shown below:

$$U_1 = \frac{3}{8}(Q_{xx} + Q_{yy}) + \frac{1}{4}Q_{xy} + \frac{1}{2}Q_{ss}$$

$$U_4 = \frac{1}{8}(Q_{xx} + Q_{yy}) + \frac{3}{4}Q_{xy} - \frac{1}{2}Q_{ss} \qquad [5.1]$$

$$U_5 = \frac{3}{8}(Q_{xx} + Q_{yy}) + \frac{1}{4}Q_{xy} + \frac{1}{2}Q_{ss}$$

The quasi-isotropic Young modulus, Poisson ratio and shear modulus of the laminates are functions of the invariants:

$$E^{[\text{iso}]} = \frac{D}{U_1},\ \nu^{[\text{iso}]} = \frac{U_4}{U_1},\ G^{[\text{iso}]} = U \qquad [5.2]$$

where $D = U_1^2 - U_4^2$.

On the other hand, when the degree of anisotropy of a composite ply increases to the upper limit, the only dominant stiffness component is the longitudinal Young modulus E_x. The matrix-related components become vanishingly small. Then the invariants above approach:

$$U_1 = \frac{3}{8}E_x,\ U_4 = \frac{1}{8}E_x,\ U_5 = \frac{1}{8}E_x \qquad [5.3]$$

The resulting engineering constants of this limiting quasi-isotropic laminate are:

$$\nu^{[\text{iso}]} = \frac{1}{3},\ G^{[\text{iso}]} = \frac{1}{8}E_x,\ D = \frac{1}{8}E_x{}^2,\ E^{[\text{iso}]} = \frac{1}{3}E_x \qquad [5.4]$$

The mathematical results in the last equation may be explained physically by viewing a laminate having three independent plies of equal thickness. The effective stiffness is equal to $\frac{1}{3}$ of the unidirectional stiffness because each ply occupies $\frac{1}{3}$ of the total laminate thickness. Having the same stiffness in 60° intervals, the laminate becomes isotropic. This can be shown by averaging the transformed stiffness components.

Using the same explanation, the stiffness of a [0/90] laminate along the 1- and 2-axes is half the longitudinal stiffness. This square symmetric network is square symmetric, but not isotropic.

5.4.2 Stiffness of isogrids

A composite isogrid is portrayed in Fig. 5.2 as a regrouped laminate where the matrix stiffness is approaching zero. The same $\frac{1}{3}$ factor in Equation 5.4 can be applied for the contribution of rib stiffness to the isogrid stiffness. This global stiffness, however, must be weighted by the area fraction f. This factor is proportional to the ratio of width b and spacing L of each rib. The Poisson ratio can also be shown to have the same value of $\frac{1}{3}$ as a laminate without matrix. A straightforward but rigorous derivation of the Poisson ratio of an isogrid as a truss will lead to this special value. The following global Young modulus and Poisson ratio of an isogrid are easy to use and to remember:

$$E^{[\text{isogrid}]} = \frac{f}{3} E_x = \frac{2}{\sqrt{3}} (L/b) E_x;\ \nu^{[\text{isogrid}]} = \frac{1}{3} \qquad [5.5]$$

where b = rib width and L = rib length as per the relations in Fig. 5.4. For square grids, the relation between the global stiffness and area fraction f or slenderness ratio L/b will be different (Section 4.3).

The relations here apply to interlaced isogrids where all the ribs are in the same plane. For stacked joint grids, ribs of different orientations run in different planes and yield an effective stiffness lower than that of interlaced grids having the same overall rig geometry. The global thickness of the grid is the sum of the rib thicknesses. The effective stiffness of such grids would be lower than that of interlaced grids having the same rib geometry. If we use the in-plane stiffness matrix [A] where the unit is N/m there is no difference between interlaced and stacked joint grids. This is an 'absolute' stiffness rather than a normalized one, the unit of which is Pa (N/m^2).

The grid stiffness depends on the rib stiffness and geometry. It can be shown that the detail of the joint at rib intersections, which can be either pinned or fixed, does not affect the grid stiffness if the slenderness ratio is high. This is the case when the area fraction is small. This will not be the case of a grid that looks like a waffle plate.

When ply anisotropy in a composite is moderate, like that of E-glass/epoxy composite, the matrix-related components are no longer negligible. The quasi-isotropic laminate stiffness will obey the relations in Equation 5.2. A comparison of laminate and grid stiffness for different materials is listed in Table 5.1. For comparison among different grid materials, the area fraction correction is the same. Its effect is included in this

Table 5.1. Comparison of stiffness of isotropic laminates and isogrids for three materials on absolute and specific bases

	Properties	Units	Source	T300/5208	Glass/epoxy	Aluminum
	E_X	GPa	Ply data [4]	181.00	38.60	70.00
	E_Y	GPa	Ply data [4]	10.30	8.27	70.00
	ν_x	GPa	Ply data [4]	0.28	0.26	0.30
	E_S	GPa	Ply data [4]	7.17	4.14	26.90
A	$\rho^{[iso]}$		Ply data [4]	1.60	1.80	2.60
B	$\rho^{[isogd]}$		$F\rho^{[iso]}$	1.60 *f*	1.80 *f*	2.60 *f*
C	$E^{[iso]}$	GPa	Equation 5.2	69.70	19.00	70.00
D	$E^{[isogd]}$	GPa	$fE_X/3$	60.30 *f*	12.90 *f*	23.33 *f*
E	$E^{[iso]}/\rho^{[iso]}$	GPa	C/A	43.56	10.55	26.92
F	$E^{[isogd]}/\rho^{[isogd]}$	GPa	D/B	37.68	7.17	8.97
G	$\text{Efficiency}^{[isogd]/[iso]}$		F/E	0.87	0.68	0.33

table; i.e. for a given fraction *f*, the global stiffness is this factor multiplied by the Young modulus shown in the table. Relative efficiencies between the grid and laminate are shown. Highly anisotropic material such as carbon fiber reinforced plastic (CFRP) is most efficient; the isotropic material is the least efficient.

Thus comparison of the stiffness ratio between grids and laminates is a measure of the efficiency of grids. The most efficient rib stiffness is the longitudinal Young modulus E_x. Aluminum and other isotropic materials cannot compete in terms of efficiency. When the mass of the materials is factored in, as in the specific stiffness, composite grids can even be more effective than metallic ones. This is shown in Fig. 5.8. Note that glass grid is nearly as efficient as aluminum grid. We can also claim that if metals must be used, keep them in plate form and add composite grid as a hybrid construction. That would be preferable to adding a metallic grid to the construction. The manufacturing process for hybrid grid/plate combination must still be developed.

5.4.3 Stiffness of square grids and cross-ply laminates

Stacked joint grids are most easily made with two orthogonal members. They are orthogrids. The stiffness comparison of orthogrids with cross-ply laminates is analogous to that of isogrids with quasi-isotropic laminates. We will compare the simplest case of an orthogrid and a cross-ply laminate by making them square constructions, i.e. the longitudinal and cross-members have the same stiffness contribution to the grid; the [0] and [90] plies of the cross-ply laminates are equal. Like Equation 5.5, we have the following relation for square grids:

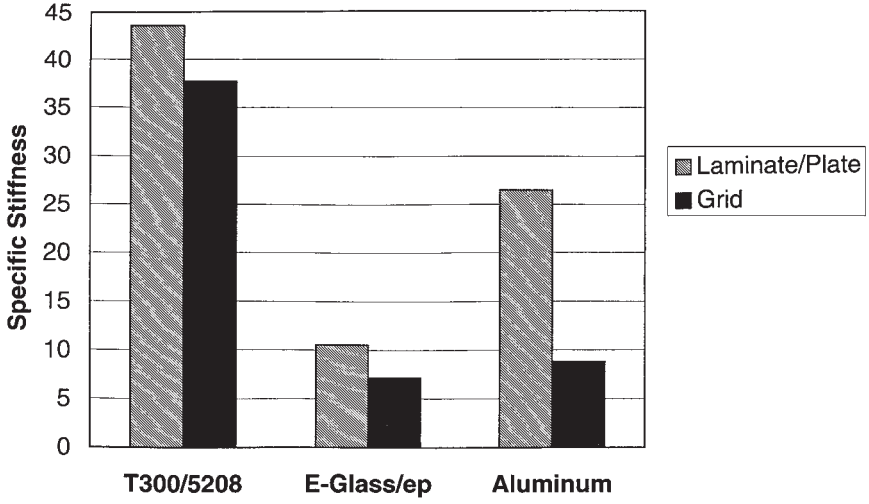

5.8 Specific stiffness of quasi-isotropic laminates and isogrids for CFRP, glass fiber reinforced plastic (GFRP) and aluminum.

Table 5.2. Comparison of stiffness of cross-ply laminates and square grids for three materials on absolute and specific bases

	Properties	Units	Source	T300/5208	Glass/epoxy	Aluminum
A	$\rho^{[iso]}$		Ply data [4]	1.60	1.80	2.60
B	$\rho^{[isogd]}$		$F\rho^{[iso]}$	1.60 *f*	1.80 *f*	2.60 *f*
C	$E_1^{[0/90]}$	GPa	Laminated plate theory [4]	96.00	23.60	70.00
D	$E_1^{[sqgd]}$	GPa	$fE_X/2$	90.50 *f*	19.30 *f*	35.00 *f*
E	$E_1^{[0/90]}/\rho^{[0/90]}$	GPa	C/A	60.00	13.11	26.92
F	$E_1^{[sqgd]}/\rho^{[sqgd]}$	GPa	D/B	56.56	10.72	13.46
G	Efficiency$^{[sqgd]/[0/90]}$		F/E	0.94	0.82	0.50

$$E_1^{[sqgrid]} = E_2^{[sqgrid]} = \frac{f}{2}E_x = \frac{b}{L}E_x;\ \nu^{[sqgrid]} = 0 \qquad [5.6]$$

The zero Poisson ratio is based on the two orthogonal ribs which are completely independent. Since there is no coupling, Poisson's ratio vanishes. The same comparisons as those made in Table 5.1 are given in Table 5.2 for square grids versus cross-ply laminates for the same materials. Square grids and cross-ply laminates are not isotropic even though the properties in two orthogonal directions are equal. Relative efficiencies between the grid and laminate are shown. Again, the more anisotropic material like CFRP becomes more efficient; the isotropic grid is the least efficient. The

Table 5.3. Comparison of stiffness of [±45] laminates and angle grids for three materials on absolute and specific bases

	Properties	Units	Source	T300/5208	Glass/epoxy	Aluminum
A	$\rho^{[iso]}$		Ply data [4]	1.60	1.80	2.60
B	$\rho^{[isogd]}$		$F\rho^{[iso]}$	1.60 *f*	1.80 *f*	2.60 *f*
C	$E_6^{[\pm 45]}$	GPa	LPT [4]	46.59	10.80	26.90
D	$E_6^{[angd]}$	GPa	$fE_x/4$	45.25 *f*	9.65 *f*	15.50 *f*
E	$E_6^{[\pm 45]}/\rho^{[\pm 45]}$	GPa	C/A	29.12	6.00	10.35
F	$E_6^{[angd]}/\rho^{[angd]}$	GPa	D/B	28.28	5.36	6.73
G	$\text{Efficiency}^{[angd]/[\pm 45]}$		F/E	0.97	0.89	0.65

elastic constants and specific gravity of the materials can be found in Table 5.1.

5.4.4 Stiffness of angle grids and [±45] laminates

A cross-ply laminate can be rotated by 45° to become an angle-ply laminate of [±45]. A square grid can also be rotated to form an angle grid with ±45° ribs. In fact, the International Space Station hull has this angle grid design. For square grids, the stiffness components in the 1- and 2-axes are equal and their value is $E^{[sqgrid]} = f/2\ E_x$ as shown in Equation 5.6. If we apply the transformation relation of 45° from the 1- and 2-axes of the square grid, we can easily show that:

$$E^{[angrid]} = \frac{1}{2} E^{[sqgrid]} = \frac{f}{4} E_x \qquad [5.7]$$

A comparison of the stiffness ratios of the three materials is given in Table 5.3. The same trend in efficiency prevails for this angle grid as well. The efficiency for aluminum reaches a value of 0.65 which is higher than 0.5 and 0.33 for square and isogrids, respectively. But it is still lower than T300/5208 composites by a wide margin in both absolute and specific values. It is still not competitive if aluminum [±45] ribs in a grid are used to increase the shear rigidity. The elastic constants and specific gravity of the materials can be found in Table 5.1.

5.5 Failure envelopes of grids

Failure envelopes for composite laminates can be based on a number of criteria; among the more common are the maximum strain and quadratic criteria. Since grids are modeled as ribs connected by hinges at the rib joints, the failure envelopes for grids are based on the lowest of three possible failure modes applied to the ribs: tensile strength, compressive strength or

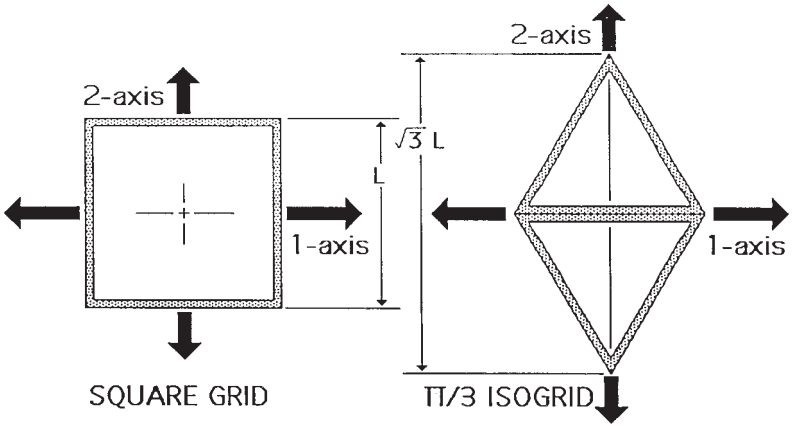

5.9 Combined normal strains or stresses for square and isogrids.

buckling. Since there is no biaxial effect on the failure of ribs, the maximum strain or maximum stress criterion seems most appropriate.

Failure of the joints is not included in the present study. It is not expected to affect the compressive strength of the grid. For tensile and shear loading conditions, joints may have lower strengths. Whether joint strength controls the grid strength or not needs to be examined in the future.

As is the case with failure envelopes for composite laminates, they can be shown in either strain or stress space. Strain space representation has the advantage of being invariant. The failure envelopes depend then only on ply orientation, not on the stacking sequence of the plies in the laminate. A [0] ply will retain its envelope in strain space whether or not there are other plies present with different orientations. Laminates having different ply orientations can be examined simply by superposing the envelopes of the desired orientations.

5.5.1 Failure envelopes in strain space

Failure envelopes in normal strain or ε_1–ε_2 space can be constructed from a state of combined strains or stresses for square and isogrids, shown in Fig. 5.9. The simplest construction is the tensile failure strain along the 1-axis:

$$\varepsilon_1 = \frac{X}{E_x} = x$$

$$\text{for T300/5208:}\quad \varepsilon_1 = \frac{1500}{181} = 8.3 \qquad [5.8]$$

$$\text{for E-glass/epoxy:}\quad \varepsilon_2 = \frac{1062}{38.6} = 27.5$$

where x is the failure strain ($\times 10^{-3}$) along the rib as shown on the left in Fig. 5.9. Since the Poisson ratio of square grids, like cross-ply laminates, is practically zero, there is no interaction due to combined strains. Failure strains form a square envelope in strain space for square grids.

For the [0] rib, the failure strain is controlled by the net strain along the 1-axis. Straining along this axis translates directly into the strain in the [0] rib. Straining along the 2-axis results in Poisson's strain along the 1-axis. The sum of these combined strains yields the net strain. When the net strain reaches the value of x, failure in the [0] rib occurs. Thus, the failure strain is a vertical line for either the tensile or compressive strain along the 1-axis, for both square and isogrids, as given by Equation 5.8.

For isogrids shown on the right of Fig. 5.10, we must determine the failure strain along the [±60] ribs in addition to that along the [0] rib. Failure strain along the 2-axis must be transformed into the normal strains along the rib axes. This strain transformation is straightforward. We can also rationalize the failure strain along the 2-axis by considering first the failure under hydrostatic strains, i.e. when the two normal strains are equal. The failure strain must be equal to x for hydrostatic tension and x' for hydrostatic compression. If we recall from Equation 5.5 that the Poisson ratio of the isogrid is $\frac{1}{3}$, it is a simple geometric problem to establish the failure strains along the 2-axis. The failure strain is $\frac{4}{3}\,x$ and $\frac{4}{3}\,x'$ for tension and compression, respectively. The geometric relations are shown on the right of Fig. 5.10. The [±60] rib fails at an applied tensile strain along the 2-axis equal to:

$$\varepsilon_2 = \frac{4}{3}\frac{X}{E_x} = \frac{4}{3}x;$$

$$\text{for T300/5208:}\quad \varepsilon_2 = \frac{4}{3} \times 8.3 = 11.0 \qquad [5.9]$$

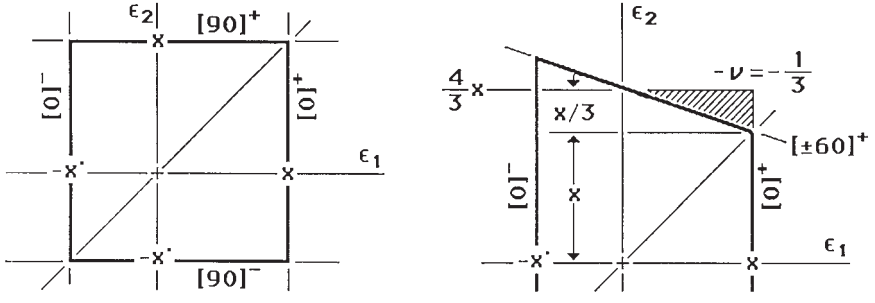

5.10 Construction of failure envelopes in strain space for square and isogrids. Ultimate tensile and compressive strains are shown as x and x', respectively.

$$\text{for E-glass/epoxy: } \varepsilon_2 = \frac{4}{3} \times 27.5 = 36.7$$

where strain is $\times 10^{-3}$.

5.5.2 Failure envelopes in stress space

Failure envelopes in stress or stress-resultant space can be derived directly from those in strain space by applying stress–strain relations. For square grids where the Poisson ratio is zero, the rectangular envelope in one space translates directly into that in the other space. This is shown on the left of Fig. 5.10. The intercepts of the failure envelopes by the 1-axis are

$$\sigma_1 = \frac{N_{1cr}}{h} = \frac{f}{2}X = \frac{b}{L}X;\ \sigma_1' = \frac{N_{1cr}'}{h} = \frac{f}{2}X' = \frac{b}{L}X' \qquad [5.10]$$

where N_{1cr}, N_{1cr}' = maximum tensile and compressive stress resultants; X, X' = tensile and compressive strengths of the unidirectional rib, respectively, h = total grid thickness. The intercepts by the 2-axis have the same corresponding numerical values as those in Equation 5.10.

The envelope for isogrids is shown on the right of Fig. 5.11. The relations corresponding to Equation 5.10 are:

$$\sigma_1 = \frac{N_{1cr}}{h} = \frac{f}{3}X = \frac{2b}{\sqrt{3}L}X;\ \sigma_1' = \frac{N_{1cr}'}{h} = \frac{f}{3}X' = \frac{2b}{\sqrt{3}L}X' \qquad [5.11]$$

The definitions are the same as those for Equation 5.10. For isogrids these intercepts apply to the 1-axis only. For the 2-axis or for a uniaxial stress applied in the [±60] ribs, the ultimate values are different. They can also be derived from the stress–strain relations of the isogrid. For example, the [0] rib is controlled by a constant strain x in the 1-axis for any value of strain

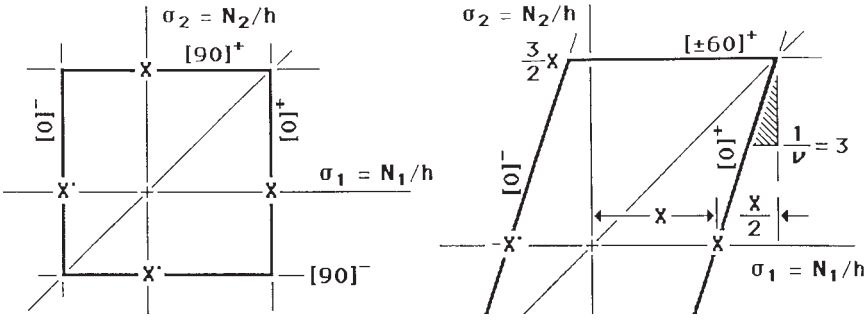

5.11 Construction of failure envelopes in stress space for square and isogrids. Ultimate tensile and compressive strengths are shown as X and X', respectively.

in the 2-axis as shown on the right of Fig. 5.10. We can write the following stress–strain relation:

$$\varepsilon_1 = a_{11}N_1 + a_{12}N_2 = X \qquad [5.12]$$

We can differentiate this equation and find that

$$\frac{\partial N_2}{\partial N_1} = -\frac{a_{11}}{a_{12}} = \frac{1}{\nu} \qquad [5.13]$$

The same result can be obtained when the applied stress is compressive. In this case, the ultimate compressive strain x' must be used in Equation 5.12.

We recognize that this [0] failure boundary intercepts the hydrostatic tensile and compressive points where ribs of any orientation must converge. Using a value of $\frac{1}{3}$ for the Poisson ratio, the coordinates of these focal points are $+\frac{3}{2}X$ and $\frac{3}{2}X'$ for tensile and compressive pressure, respectively.

We can rationalize the tensile or compressive failure of [±60] ribs by stress applied along the 2-axis. The failure by stress in these ribs is a function of the rib orientations. Any stress applied along the 1-axis changes these orientations only slightly. Thus the strength along the 2-axis remains constant, independent of the stress applied, along the 1-axis. The externally applied stresses on an isogrid can be seen in Fig. 5.9. The controlling envelope in stress space appears as horizontal lines on the right of Fig. 5.11. The values of the intercepts by the 2-axis are $+\frac{3}{2}X$ and $-\frac{3}{2}X'$.

5.5.3 Failure by rib buckling

When the applied stress or strain is in compression, the rib can fail in either one of two modes: compressive strength or Euler buckling. We have just covered the former failure mode. The other rib failure mode can be most easily described by Euler buckling. The critical axial compressive load P_{cr} and ε_{cr} for the rib are:

$$P_{cr} = \frac{\pi^2 El}{L^2} = \frac{\pi^2 Ehb^3}{12L^2}$$
$$\varepsilon_{cr} = \frac{P_{cr}}{EA} = \frac{P_{cr}}{Ehb} = \frac{\pi^2}{12(L/b)^2} \qquad [5.14]$$

where E = rib axial stiffness, L = rib length, l = moment of inertia = $hb^3/12$, b = rib width, h = rib height, A = rib cross-section = hb. It is assumed that $h > b$, thus buckling occurs by bending the width b of the rib.

Each rib will buckle when a critical Euler strain is reached in it. The critical rib slenderness for buckling of grids is easily deduced from Equation 5.14:

$$\left(\frac{L}{b}\right)_{cr} = \frac{\pi}{\sqrt{(12x')}}$$

$$\text{for T300/5208: } \left(\frac{L}{b}\right)_{cr} = 10.0 \qquad [5.15]$$

$$\text{for E-glass/epoxy: } \left(\frac{L}{b}\right)_{cr} = 7.2$$

In terms of area fraction *f*, Equation 5.14 is rewritten as follows. For isogrids, we obtain:

$$\varepsilon_{cr} = \frac{P_{cr}}{EA} = \left(\frac{\pi f}{12}\right)^2, \text{ where } f = 2\sqrt{3}\left(\frac{L}{b}\right) \qquad [5.16]$$

For square grids, we obtain:

$$\varepsilon_{cr} = \frac{P_{cr}}{EA} = \frac{(\pi f)^2}{48}, \text{ where } f = \frac{2}{(L/b)} \qquad [5.17]$$

Equations 5.16 and 5.17 can be rearranged to determine the critical area fraction *f* when the compressive failure strain and Euler buckling strain are equal. When fraction *f* is greater than this critical value, ribs fail under compressive strain. When fraction *f* is smaller than this critical value, ribs fail by buckling. Rewriting Equation 5.16 to determine the critical area fraction for isogrids,

$$f_{cr} = \frac{12}{\pi}\sqrt{x'} = 3.82\sqrt{x'}$$

$$\text{for T300/5208: } f_{cr} = 0.35 \qquad [5.18]$$

$$\text{for E-glass/epoxy: } f_{cr} = 0.48$$

Rewriting Equation 5.17 for the critical area fraction for square grids,

$$f_{cr} = \frac{\sqrt{48}}{\pi}\sqrt{x'} = 2.2\sqrt{x'}$$

$$\text{for T300/5208: } f_{cr} = 0.20 \qquad [5.19]$$

$$\text{for E-glass/epoxy: } f_{cr} = 0.28$$

We can now define waffle plates as those where rib buckling does not occur. In fact the critical value for area fraction can also be viewed as the minimum value; i.e. $f_{cr} = f_{min}$ if rib buckling is to be prevented. For T300/5208 waffle grids, this area fraction *f* has to be larger than 0.35 for isogrids and 0.20 for square grids. The corresponding values for E-glass/epoxy are 0.48 and 0.28, respectively. Glass being less stiff than graphite, the higher area fraction or denser grid for rib buckling is expected.

The buckling strain is thus proportional to the square of the area fraction. For example, if the area fraction f is reduced by a factor of 1.41 or $\sqrt{2}$, the failure strain is reduced by one half. This is shown in Fig. 5.12 where the wavy lines represent rib buckling due to the reduced area fraction for square grids. The buckling controlled failure envelopes are designated by a superscript 'b' for rib buckling. The envelopes on the left are in strain space; on the right, in stress space. If the material is T300/5308 and the area fraction is $f = f_{cr}$, the new area fraction f becomes $f = 0.20/\sqrt{2} = 0.14$.

The envelopes in strain and stress space for isogrids are shown in Fig. 5.13. The buckling envelopes are again shown as wavy lines. The area fraction f that initiates rib buckling for T300/5208 is 0.35 as stated in Equation

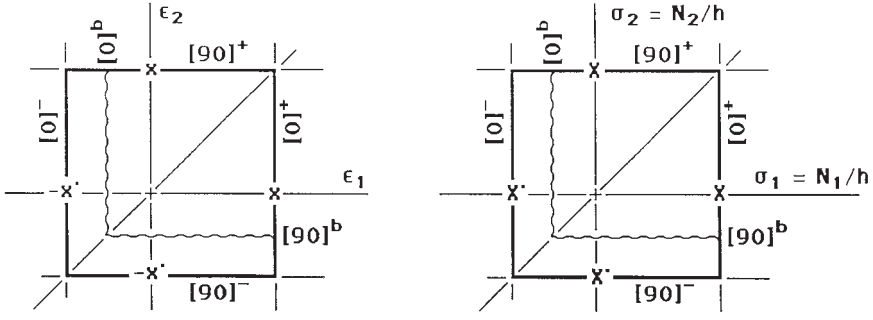

5.12 Failure envelopes in strain- and stress-resultant space for a square grid. The solid lines represent failure by tensile or compressive strains/stresses; the wavy lines represent rib buckling.

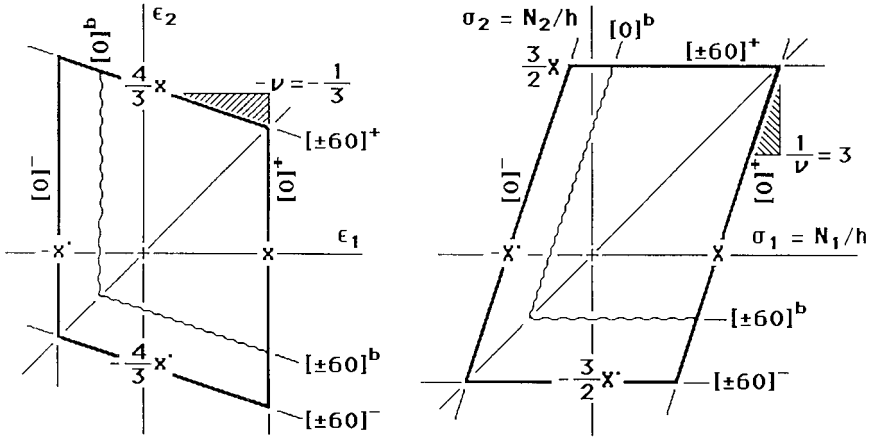

5.13 Failure envelopes in strain- and stress-resultant space for an isogrid. The solid lines represent failure by tensile or compressive strains/stresses; the wavy lines represent rib buckling.

5.18. The displayed inner buckling lines are defined by a reduction in the area fraction by a factor of 1.41 or $\sqrt{2}$; i.e. down to $f = 0.35/\sqrt{2} = 0.25$. The envelopes for compressive strains and stresses are again reduced by one half.

5.5.4 Examples of CFRP and GFRP failure envelopes

In Fig. 5.13, we show the failure envelopes of isogrids in the normal strain space for T300/5208 graphite/epoxy and E-glass/epoxy composites. These envelopes are the same as the envelope on the left of Fig. 5.13 drawn to scale. For the T300/5208 envelope, shown on the left of Fig. 5.14, the critical area fraction $f_{cr} = 0.35$. Compressive failure will be determined by strength when $f \geq 0.35$. Alternatively we can set $f_{cr} = f_{min}$ so that rib buckling will not occur. Two lower area fractions of 0.28 and 0.23 are shown as successively contracting envelopes resulting from rib buckling.

For E-glass/epoxy isogrids, the critical area fraction is $f_{cr} = 0.48$, shown in Equation 5.17. When area fractions are less than this critical value, rib buckling will occur; i.e. $f \leq f_{min}$. Two such lower area fractions of 0.35 and 0.28 are shown for an E-glass/epoxy grid on the right of Fig. 5.14.

Comparing the two envelopes in Fig. 5.14, the E-glass strain envelope is much larger. Glass fibers have larger strain capability than graphite. The difference is about three times in favor of the glass composite grid. In terms of stress, glass grids are not as strong as graphite grids. The modes of failure, however, are similar. The tensile, compressive and buckling failures follow the same pattern as those for graphite grids.

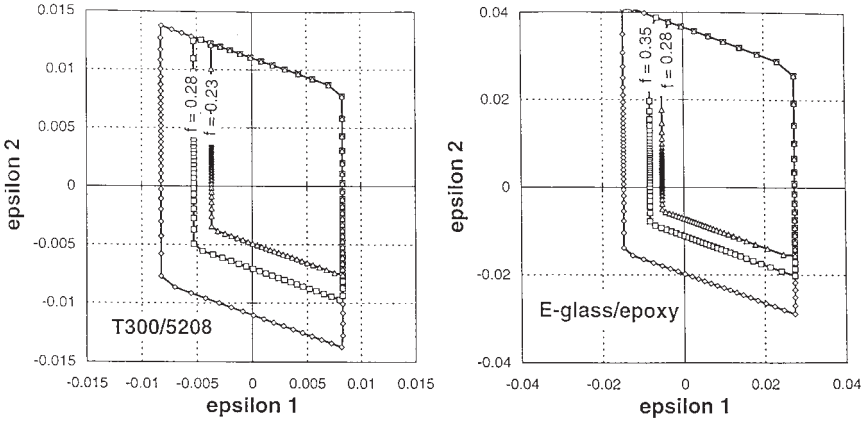

5.14 Failure envelopes of T300/5208 and E-glass/epoxy isogrids in normal strain space. Rib buckling occurs when area fraction *f* becomes less than a critical value as shown by the two inner envelopes.

Since glass is less stiff than graphite, the buckling occurs in shorter ribs or larger area fraction. The difference, for example, is $(L/b)_{cr} = 10.0$ or $f_{cr} = 0.35$ for T300/5208 and $(L/b)_{cr} = 7.2$ or $f_{cr} = 0.48$ for E-glass/epoxy.

5.6 Grids with skins

Grids can also have one or two skins. While we believe that grids are completely capable of carrying the applied external in-plane and flexural loads, skins can either share the load and/or perform functions like containing pressure or preventing penetration of an unwanted object. Interaction between skins and grids makes their combination not as simple as grids by themselves. The combination means the construction of two or more different material forms is no longer macroscopically homogeneous. The interaction of different material forms must be examined on a case by case basis. Buckling of ribs is constrained by the skins. Skin buckling is an added failure mode. Chen and Tsai [2] described various buckling failure modes.

If we treat the grid and skins as two materials, the resulting in-plane stiffness follows the rule of mixtures. Because the density of the grid is much lower than that of the solid skins, the stiffness on a weight basis is different from that on a volumetric basis. This difference is analogous to the fiber fractions of a composite where the weight fraction is higher than the volume fraction. As a result, the relative performances of grids with and without skins are different on weight and volume bases. We have not been able to establish general rules.

For simplicity, we examine only grids with two identical, symmetric skins. We purposely limit our illustration to an isotropic grid/skin construction with equal thicknesses; i.e. each quasi-isotropic skin is a quarter and the isogrid is half the total thickness. Failure envelopes are limited to in-plane loading only and are shown in absolute or normalized stress resultant. Each representation conveys different information on the behavior of the grid/skins construction.

5.6.1 CFRP grid with laminated skins

In Fig. 5.15, we show on the left two envelopes in stress-resultant space. First, a T300/5208 isogrid without rib buckling ($f \geq f_{cr} = 0.35$) is shown. For $f = f_{cr}$, the weight of the grid equals 35% that of the skins, or approximately 25% the total weight. On the same side of this figure, the first failure (FF) envelope of an isogrid with quasi-isotropic laminated skins is shown. In the first, second and fourth quadrants, the grid has higher strength capability:

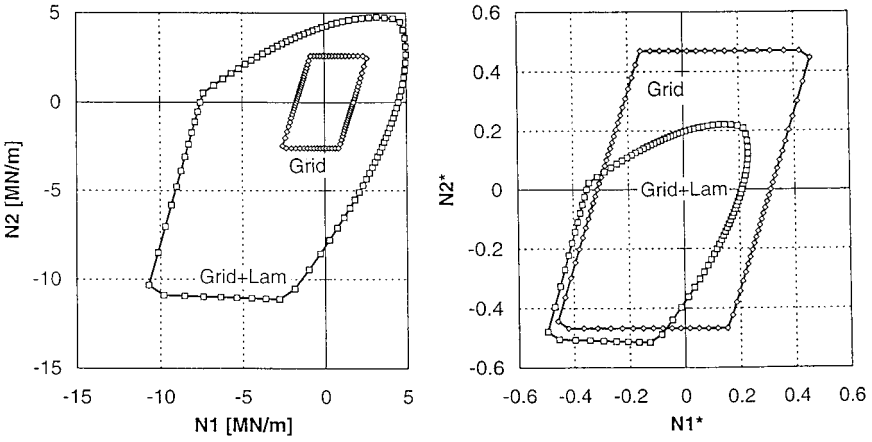

5.15 Failure envelopes of T300/5208 isogrid with quasi-isotropic skins in absolute and specific stress-resultant space.

the laminate defines the first failure (FF) envelope. In the third quadrant, the laminate is stronger. The grid defines the FF envelope.

While the grid envelope is diminutive as compared with the grid and skins, the substantial difference in weight must be considered. To compensate for this difference, the failure envelopes are plotted in specific stress-resultant space shown on the right of Fig. 5.15. The normalization is done by dividing the stress resultant by the total weight of the structure. In this figure, the grid envelope is enlarged about four times (1/0.25) relative to the FF of grid with skins. This figure may help to visualize the respective capabilities of grid alone and grid/skin combination.

5.6.2 GFRP grid with laminated skins

The same comparison between grid and grid/skin is made for E-glass/epoxy material. For the same absolute and specific stress-resultant representations, the failure envelopes of E-glass/epoxy grids and skins are shown in Fig. 5.16. The critical area fraction for this material is 0.48. So the grid weighs 48% the weight of the skins, or 32% of the total. In absolute space, shown on the left of this figure, the FF envelope of the grid and skins combination is again much larger than that of the grid alone.

When the relative weight is taken into account as is the case in the specific stress-resultant representation on the right of Fig. 5.16, the grid shows much greater strength capability. Thus the first failure is determined by the weaker of the two components. In this case, it is the laminate that limits the entire FF envelope.

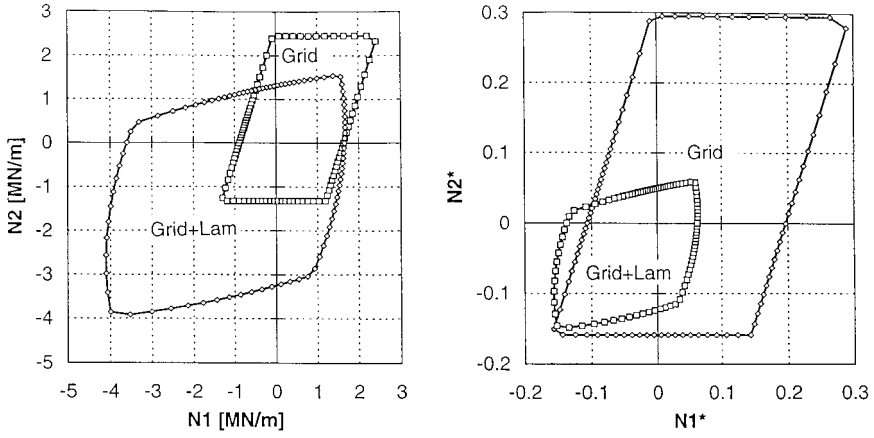

5.16 Failure envelopes of E-glass/epoxy isogrid with quasi-isotropic laminated skins in absolute and specific stress-resultant space.

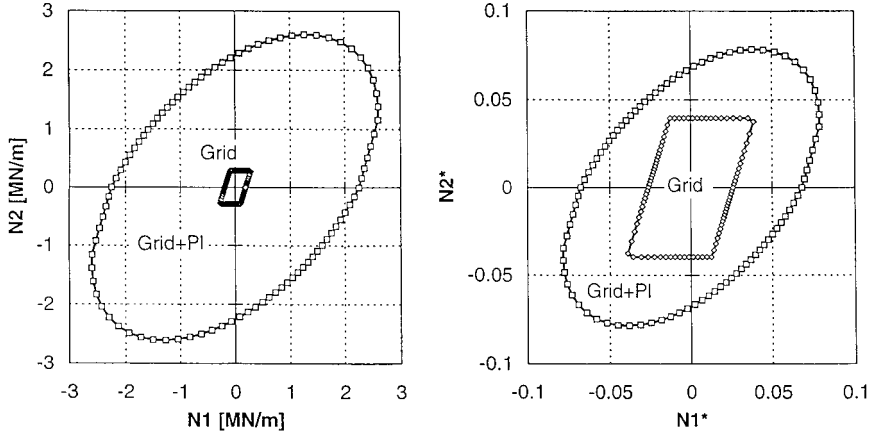

5.17 Failure envelopes of aluminum grid with skins in absolute and specific stress-resultant space.

5.6.3 Aluminum grid with skins

For aluminum grids with skins, the FF envelope is larger than the grid envelope everywhere. The grid fails at significantly lower stresses. They are shown in absolute and specific stress-resultant spaces in Fig. 5.17. Thus metallic grids are not only less stiff than skins, they are weaker by a wide margin as well. Metallic grids are not recommended for applications where either stiffness or strength is critical. There must be other reasons to justify their use.

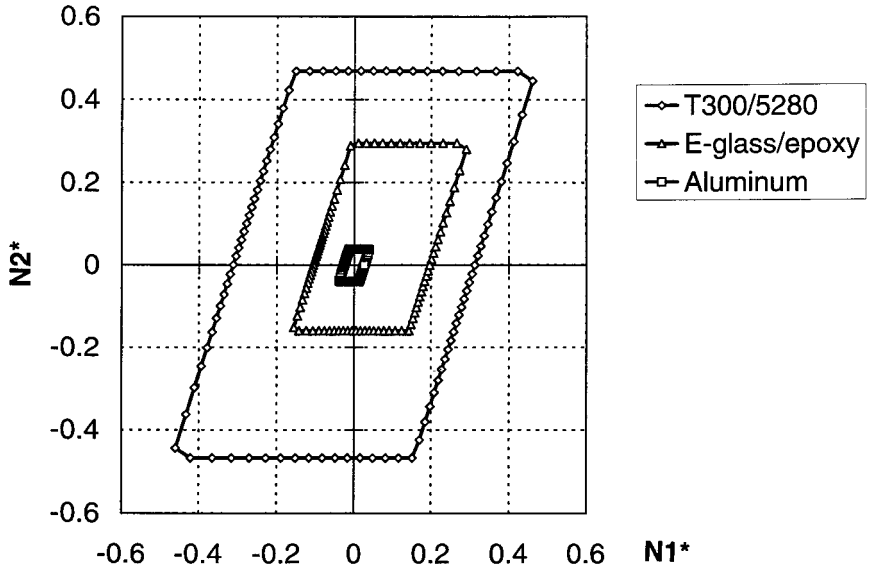

5.18 Comparison of three grids in specific stress space. The ranking is as follows: CFRP, GFRP and aluminum.

To make a meaningful comparison of failure envelopes in stress-resultant space, we use specific strength. The grids here do not have skins. The higher the specific strength, like specific stiffness, the more efficient the material in its load-carrying capability per unit weight. This is shown in Fig. 5.18.

We have tried to show that grids have strong interaction in combination with skins. It must be assessed on a case-by-case basis. It is, however, clear that composite grids have superior strength and should be utilized to maximum extent. Metallic grids are not efficient and must only be used after careful consideration.

Grids present a challenge for the designers. As we improve our understanding of the behavior of grids, with or without skins, we should now explore hybrid combinations such as composite grids with metallic face sheets. It may be feasible to design a structure with specific properties not possible otherwise with conventional constructions.

5.7 Flexural rigidity of isogrids

As stated earlier, the flexural rigidity of grids follows the same cubic relation with the grid height as the thickness of solid plates and laminates. In addition, rigidity [D] of isogrids is directly proportional to the area fraction f. Since the mass of the grid is also proportional to this area fraction, the

specific flexural rigidity ($[D^*] = [D]/\text{mass}$) will remain the same as the fraction changes.

The poor conversion of rib to grid for the in-plane stiffness is carried over to the flexural rigidity. Again, we wish to emphasize that metallic grids are not effective. The examples in the following are intended to illustrate this point.

5.7.1 Flexural rigidity of a CFRP isogrid

Find $[D]$ and $[D^*]$ for a T300/5208 graphite/epoxy isogrid.

Case 1

The grid dimensions are: rib height 10 mm, rib width 4 mm, rib length 50 mm.

$$\text{Area fraction: } f = 0.28 \quad \text{Mass per area} = 4.43\,\text{kg/m}^2 \qquad [5.20]$$

$$\text{Flexural rigidity: } D_{11} = D_{22} = 1577\ \text{N m},\ D_{66} = 532\ \text{N m} \qquad [5.21]$$

$$\text{Specific flexural rigidity: } D_{11}^* = D_{22}^* = 356\,\text{N m/(kg/m}^2) \qquad [5.22]$$

$$D_{66}^* = 120$$

Case 2

If the rib width is reduced from 4 to 2 mm

$$\text{Area fraction: } f = 0.14 \quad \text{Mass per area} = 2.21\,\text{kg/m}^2 \qquad [5.23]$$

$$\text{Flexural rigidity: } D_{11} = D_{22} = 785\ \text{N m},\ D_{66} = 263\ \text{N m} \qquad [5.24]$$

$$\text{Specific flexural rigidity: } D_{11}^* = D_{22}^* = 354\,\text{N m/(kg/m}^2) \qquad [5.25]$$

$$D_{66}^* = 118$$

The slight difference in the specific $[D^*]$ is caused by the contribution from the twisting rigidity of the ribs which is not proportional to the rib width.

Case 3

If a quasi-isotropic laminate [0/+60/–60] of the same height (10 mm) is added symmetrically to the grid, there are 80 plies.

$$\text{Area fraction: } f = 0.28 \quad \text{Mass per area} = 16\,\text{kg/m}^2 \qquad [5.26]$$

$$\text{Flexural rigidity: } D_{11} = D_{22} = 6364\ \text{N m},\ D_{66} = 2240\ \text{N m} \qquad [5.27]$$

$$\text{Specific flexural rigidity: } D_{11}^* = D_{22}^* = 397\,\text{N m/(kg/m}^2) \qquad [5.28]$$

$$D_{66}^* = 140$$

There is a significant increase in $[D]$ but only a modest increase in $[D^*]$.

Case 4

If the height of the grid is increased to match the weight of the previous grid + laminate combination (case 3)

Height = 36 mm

Area fraction: $f = 0.28$ Mass per area = $16\,\mathrm{kg/m^2}$ [5.29]

Flexural rigidity: $D_{11} = D_{22} = 73667\ \mathrm{N\,m}$, $D_{66} = 24585\ \mathrm{N\,m}$ [5.30]

Specific flexural rigidity: $D_{11}^* = D_{22}^* = 4604\ \mathrm{N\,m/(kg/m^2)}$ [5.31]

$D_{66}^* = 1536$

There is an order of magnitude increase in both $[D]$ and $[D^*]$.

5.7.2 Flexural rigidity of an aluminum isogrid

Find $[D]$ and $[D^*]$ for aluminum grid with the same dimensions.

Case 1

Grid dimensions: rib height 10 mm, rib width 4 mm, rib length 50 mm.

Area fraction: $f = 0.28$ Mass per area = $7.21\,\mathrm{kg/m^2}$ [5.32]

Flexural rigidity: $D_{11} = D_{22} = 633\ \mathrm{N\,m}$, $D_{66} = 236\ \mathrm{N\,m}$ [5.33]

Specific flexural rigidity: $D_{11}^* = D_{22}^* = 87.9\ \mathrm{N\,m/(kg/m^2)}$ [5.34]

$D_{66}^* = 32.7$

Case 2

A solid aluminum plate of the same height.

Height = 10 mm Mass per area = $26\,\mathrm{kg/m^2}$ [5.35]

Flexural rigidity: $D_{11} = D_{22} = 6309\ \mathrm{N\,m}$, $D_{66} = 2208\ \mathrm{N\,m}$ [5.36]

Specific flexural rigidity: $D_{11}^* = D_{22}^* = 243\ \mathrm{N\,m/(kg/m^2)}$ [5.37]

$D_{66}^* = 85$

Note that the rigidity of the grid is much lower than that of the plate for both $[D]$ and $[D^*]$.

5.8 Coefficients of thermal expansion

One unique feature of composite grids with graphite fibers is their low coefficients of thermal expansion (CTE). Five common graphite/epoxy

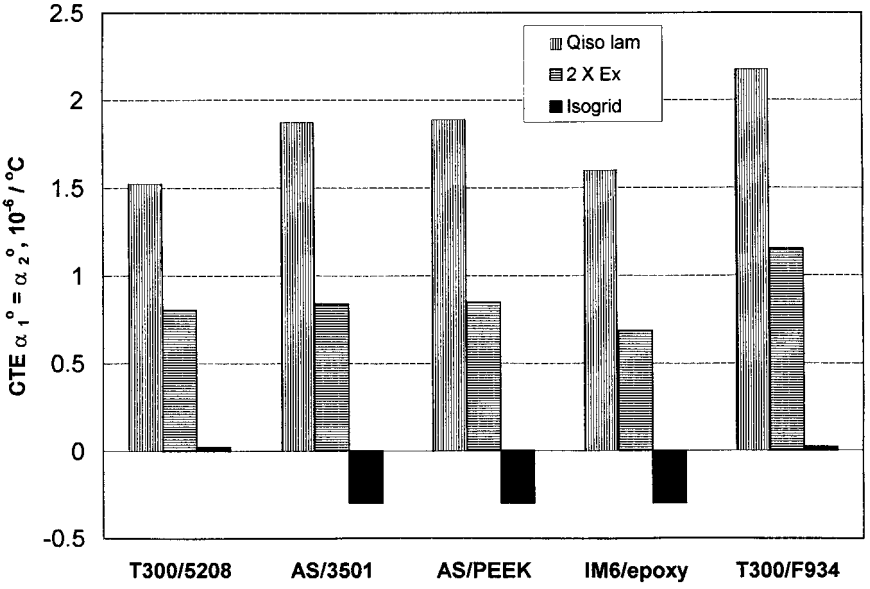

5.19 CTE of CFRP quasi-isotropic laminates and isogrids, including fictitious composites having doubled longitudinal stiffness to simulate high-modulus fibers.

composites are shown in Fig. 5.19. The first of three columns for each composite material represents the CTE of quasi-isotropic laminates. The value is between 1.5×10^{-6} and 2×10^{-6} for all the composites shown. The next column shows the CTE for the same laminate if the longitudinal Young modulus is doubled. The CTE is decreased by a factor of 2 which is a direct result of having higher modulus fibers.

The third column shows the CTE of an isogrid made of the same unidirectional composite. The value is not only significantly lower, it is near zero or even slightly negative. A negative CTE is possible for laminates in only one direction; for isogrids it is bidirectional in the plane of the grid. This unique feature of composite grids can be greatly utilized in structures for satellites.

On the other hand, the CTE for E-glass/epoxy isogrids is 11.35 which is much higher than that of graphite/epoxy composites as shown above. This CTE is very close to that of steel (12×10^{-6}). Thus from the standpoint of matching CTE, a glass/epoxy isogrid will be perfect with steel face sheets. Aluminum is even higher at about 24×10^{-6}. But the CTE mismatch between GFRP and aluminum is less severe than that between CFRP and aluminum.

5.9 Conclusions

We have tried to illustrate the unique properties and manufacturing processes offered by composite grids. If they can be produced in large quantities and sizes at low cost, such products will find markets in many fields. Most of the processes described herein can be automated. Low-cost and high-volume production are entirely feasible. Grids may emerge as a viable alternative to the conventional laminated, stiffened and/or sandwich constructions. We realize that composite grids are as simple as composite laminates.

We enthusiastically embrace grids for many applications. For glass/epoxy grids, there are opportunities in the reinforcement systems of concrete structures and piling. We also envision vessels and piping for internal and external pressures, energy absorption devices and containment rings for rotating machinery. For graphite/epoxy grids, we see low-cost structures for fuselages, and several components of launch vehicles and satellites. Having a wide range of controllable coefficient of thermal expansion available, thermal matching of support structures is possible. Dynamic tuning and damping are also easily available with composite grids. Customized structures can be made in weeks instead of months or years. We hope to continue to gain design and manufacturing experience so composite grids can be recognized as something special.

5.10 Acknowledgements

The authors wish to thank their former and current employers for the support of this work. Financial support from US Air Force Office of Scientific Research, National Science Foundation, US Army Corps of Engineers, National Renewable Energy Laboratory, Stanford Integrated Manufacturing Association, and Industrial Technology Research Institute of Hsinchu are gratefully acknowledged.

5.11 References

1. Meyer, R.R., McDonnell Douglas Astronautics Company, *Isogrid Design Handbook*, NASA Contractor Report, CIR-124075, Revision A, 1973.
2. Hong-Ji Chen, H.-J. and Tsai, S.W., 'Analysis and optimum design of composite grid structures', *J. Composite Mater.*, **30**(4/6), 503–534, 1996.
3. Huybrechts, S.M., 'Analysis and behavior of grid structures', PhD thesis, Stanford University, Department of Aeronautics and Astronautics, 1995.
4. Tsai, S.W., *Theory of Composites Design*, Think Composites, Palo Alto, CA, 1992.